J Mater Sci: Mater Med (2009) 20:1389–1399
DOI 10.1007/s10856-009-3706-4

Thermal impurity reactions and structural changes in slightly carbonated hydroxyapatite

Z. Z. Zyman · D. V. Rokhmistrov · V. I. Glushko · I. G. Ivanov

Received: 25 January 2008 / Accepted: 6 February 2009 / Published online: 10 March 2009

Abstract Lattice and surface impurity reactions and structural changes induced by them in slightly carbonated hydroxyapatite (SCHA) treated at 25–1100°C were comprehensively studied. The SCHA was processed by a conventional wet synthesis at a high possible temperature (96°C) using ammonium containing parent reagents. IR-spectroscopy, XRD, TG-DTA technique and mass spectrometric thermal analysis (MSTA) were employed for characterization of the samples. NH_4^+ with H_3O^+ in cationic- and CO_3^{2-} (A- and B-positions) with HPO_4^{2-} in anionic sites, and H_2O, CO_3^{2-}(HCO_3^-) NO_3^-, N_xH_y on the surface of particles were found and considered as impurity groups. Complicated changes in lattice constants of the SCHA stepwise annealed in air (for 2 h) were revealed; the changes were associated with reactions of the impurity groups. Filling the hexed sites with hydroxyl ions above 500°C was shown to happen partly due to lattice reactions but was mainly owing to hydrolysis of the SCHA by water molecules in air. Decomposition of CO_3^{2-} groups proceeded through both thermal destruction and reactions with some of the impurity ions. The decarbonation in A-sites occurred at much lower temperatures (450–600°C) than in B-sites (700–950°C) and was first revealed to happen in two stages: due to an impurity reaction around 500°C, and then through thermal destruction at 570°C. A redistribution of CO_3^{2-} ions, decreasing in amount on the whole, was observed upon annealing above 500°C. To avoid possible erroneous conclusions from TG-data, a sensitive method was shown to be required for monitoring gaseous decomposition products (such as the MSTA in this study), in case several impurity groups were present in a SCHA.

Z. Z. Zyman (✉) · D. V. Rokhmistrov · V. I. Glushko · I. G. Ivanov
V.N. Karazin Kharkiv National University, Kharkiv, Ukraine
e-mail: intercom@univer.kharkov.ua

1 Introduction

Hydroxyapatite, $Ca_{10}(PO_4)_6(OH)_2$, HA, has many applications, e.g., as an absorber, catalyst, gas sensor, ion filter, and predominantly, as bioactive material in biomedical fields [1–6].

One of the peculiar features of HA is its ability to accept ionic substituents and vacancies. As a consequence, the mineral part of human hard tissues contains a calcium-deficient HA (CdHA) keeping foreign ions in small or trace amounts in both cationic and anionic sites. The most frequent impurities in biological HA's are CO_3^{2-}, HPO_4^{2-}, Mg^{2+} ions and H_2O molecules. It is considered that the mineralized tissues, by absorbing foreign ions, adapt to arising physiological needs.

Impurity ions also significantly affect the functional properties of HA and HA-related materials. For instance, rates of alcohol hydration on catalysts of nonporous crystalline HA of varying Ca/P ratios correlated with increasing calcium deficiency [2]; porous HA ceramics used as gas sensors manifested increasing resistance change after soaking in certain solutions [3]; or HA-based materials in the forms of both loose powders and ceramic foams, tested with respect to their potential for removing heavy metal ions from aqueous solutions, revealed the more pure grades generally to yield the best performance [5].

Due to its many applications, HA materials with carbonate and other foreign ions were subjected to numerous studies [6, 7]. The studies often characterized how one or, rarely, two foreign pieces simultaneously effected

properties of the materials. However, processing by a simple method without special precautions (which is of great value in industrial production) usually results in a number of impurities being incorporated into a product. Therefore there has been much more contradictory than consistent data in many impurity problems. This particularly relates to altered lattice constants of HA in powders processed by a conventional wet synthesis. The alteration is especially noticeably in a constant which is usually by about 0.002 nm higher than that of HA (the reference lattice constants of stoichiometric HA are: $a = 0.9418 \pm 0.0002$ nm, $c = 0.6884 \pm 0.0002$ nm [7]). According to the most accepted explanation, the inconsistency is due to structural water incorporated into the lattice. This conclusion was derived from the observation that the enlarged constant was considerably reduced upon annealing a precipitated HA powder in air at 200–400°C when the structural water released [8].

Another "classic" impurity problem is the localization and thermal lattice reactions of carbonate ion CO_3^{2-}. The ion was assumed to be located in so called A- (substitution of OH^-) and B- (substitution of PO_4^{3-}) sites. Many lattice reactions have been considered for CO_3^{2-} decomposition. Additionally, phosphate ions may be possibly substituted for carbonate ions in a few modes [9].

Carbonated hydroxyapatites (CHA) have a lack of hydroxyl ions, thus the more the carbonation the less the ions [10]. During calcination in air, decarbonation of the apatites occur, and OH^- groups appear in the lattice again. However, no clear mechanism has been accepted for this process [6, 7].

It was recently found [11] that both lattice constants in a HA powder, processed by a wet synthesis, abruptly reduced from increased values to lower ones when heated in air within the range 25–200°C, i.e., at much lower temperatures than those in former studies [7, 8]. The reduction in lattice constants was clearly accompanied by pressure oscillation when the heat treatment was conducted in vacuo. A few correlated changes in the lattice constants and pressure were also observed in the temperature range that was usually associated with decomposition of the carbonate ion.

This study was a further attempt to ascertain the processes that result in alterations of lattice constants [11] and to discuss some results in the impurity problems noted above, especially those associated with simultaneous lattice reactions of a few foreign pieces.

2 Materials and methods

Powders were derived from a conventional wet synthesis based on the Hayek–Stadlmann reaction [7]. Three initial requirements were involved. First, no sodium contained salt was used in order to prevent Ca^{2+} for Na^+ substitution; second, no carbonate contained compound was added to the reaction mixture since enough carbonate ions were even in distilled water to enter the lattice and form an AB-type CHA [12]. Finally, the reaction was conducted at 96°C, one of the highest in wet synthesis, in order to get crystals large enough for precision determination of lattice constants.

An appropriate proportion of parent reagents was supposed to result in the stoichiometric molar ratio of Ca/P = 1.67 in the product. 2850 ml of a $(NH_4)_2HPO_4$ aqueous solution (0.34 mol l^{-1} in concentration) was slowly added to 950 ml of a $Ca(NO_3)_2 \cdot 4H_2O$ solution (1.28 mol l^{-1}) over 2 h at 96°C and pH = 10–11 (previously adjusted with NH_4OH) and the reaction mixture was stirred for 24 h. After cooling the mixture, the precipitate was alternately centrifugalized and washed 4 times. Freshly distilled water was used in preparing the solutions and washing. The completed washed precipitate was dried at room temperature (RT) for few days and the resulted powder was stored in a desiccator.

Aliquots of the powder were heated in air to 1100°C, in steps of 50°C or 100°C with 2 h dwell-time at each temperature. Samples once annealed were studied by infrared spectroscopy (IR; Specord 751, Germany) employing the conventional KBr—pellet technique. X-ray powder diffraction (XRD) was conducted in CuK_α radiation (DRON–2 M, USSR). The lattice constants a and c were measured with an accuracy better than ±0.0004 nm using the (300) and (002) reflections and aluminum as an internal standard [8]. Thermogravimetry coupled with differential thermal analysis (TG-DTA) was performed in the temperature range of 20–950°C at the heating rate of 5 K min^{-1} in air using a platinum crucible (Q—Derivatograph, Hungary). Mass spectrometric thermal analysis (MSTA) was carried out according to a known procedure [13] and using a home–made apparatus which was similar in arrangement with the one employed earlier [14]. While heating a sample in vacuo, the temperature rose at a linear rate of 5 K min^{-1} as that in TG measurements. Gaseous decomposition products of a sample passed through a calibrated leak operated by a piezoelectric crystal system (SNA-2, SELMI, Sumy, Ukraine) into the vacuum chamber of a dynamic radio frequency mass-spectrometer (MX-7304A, SELMI, Sumy, Ukraine).

3 Results and discussion

The IR spectrum of an as-processed powder (Fig. 1a) was a typical one of CHA: PO_4^{3-} bands at 478 cm^{-1} (ν_2), 563 and 603 cm^{-1} (ν_4), 965 cm^{-1} (ν_1), 1055, 1075, 1085 and 1105 cm^{-1} (ν_3); two weak shoulders at 625 and 3560 cm^{-1}

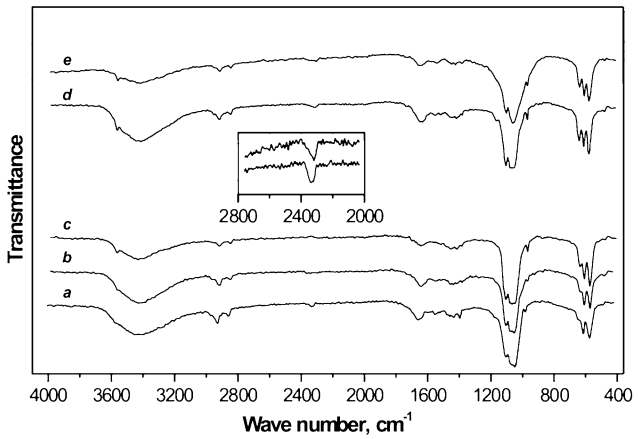

Fig. 1 IR spectra of the powders at (a) RT and annealed in air for 2 h, at: (b) 400°C, (c) 600°C, (d) 800°C, (e) 1100°C. The inset presents CO_2 -bands of the samples treated at: 500°C-below, 800°C-above. The sections are enlarged with respect to the spectra

of librational and stretching modes of OH^-, respectively; CO_3^{2-} absorbtions of v_2 (875 cm^{-1}) and v_3 domains (the last are in Table 1). The localization and, on the whole, weak intensities of the carbonate bands showed that the powder was slightly carbonated HA (SCHA) [12]. Also, a broad librational band with a top at about 3400 cm^{-1} and a sharp bone at 1640 cm^{-1} of adsorbed water, a weak absorption within 2200–2400 cm^{-1} of molecular CO_2 [15], a sharp peak of NO_3^- ion at 1385 cm^{-1}, as well as two sharp peaks at 2910 and 2845 cm^{-1} of presumably N_xH_y contamination [7] were present. Besides, there were a few weak peaks and shoulders at 1250, 1185, 920 and 865 cm^{-1} that pointed to the presence of HPO_4^{2-} ions and/or traces of octacalcium phosphate precursor in the product [16, 17]. The positions of phosphate bands during the heat treatment experienced minor changes; the main alterations were observed for carbonate and OH^- groups that are discussed further.

The temperature dependences of lattice constants a and c are shown in Fig. 2. The c value during the heat treatment displayed slight changes, but the a value changed considerably. Since the latter is much more sensitive to lattice impurities than the former in HA-based products [18], processes which occurred in samples during heating are further discussed mainly in relation to the measured a-dependence. For convenience, the dependence is divided into the following ranges: RT–500, 500–600, 600–700, 700–800, 800–1050, and 1050–1100°C.

RT–500°C. The lattice constants $a = 9.433 \pm 0.003$ Å and $c = 6.904 \pm 0.003$ Å in an as—processed powder differed from $a = 9.418 \pm 0.002$ Å and $c = 6.884 \pm 0.002$ Å of the reference (stoichiometric) HA; the last values are marked by continuous and broken lines in Fig. 2. This was expected since the corresponding IR spectrum manifested a contaminated product (Fig. 1a). Of the impurities ascertained by the spectrum, CO_3^{2-} groups in a precipitated CHA was known to cause a reduction in a and a slight increase in c values related to the

Table 1 Alterations of the bands in IR-spectra of heat-treated SCHA in the v_3 CO_3^{2-} range (1400–1600 cm^{-1})

Temperature (°C)											
RT	100	200	300	400	500	600	700	800	900	1000	1100
1585sh	1585w	1585w	1585sh	1585w			1580vw	1590mw			
1565w	1565m	1565ms	1570m	1570m	1570m	1570mw		1570w	1567m	1565sh	1570w
1540s	1550m	1545ms	1555mv	1550s	1540ms	1540s	1555ms	1555s	1543m	1540s	1545s
1530w	1530mw	1530ms	1540w	1535ms			1543w	1540m	1530mw		1530w
			1530ms								
1520sh		1515w	1515w	1515ms	1520w	1520w	1515w	1515s	1515mw	1515sh	
1505ms	1510m	1505s			1505sh		1503sh				1505w
1490vw	1490ms	1495sh	1495w	1495w		1490ms	1495ms	1497m	1490w		1495w
	1480mw		1475sh	1475m				1480m			
1465m	1460sh	1460sh	1465mv	1465sh	1460sh	1462m	1465ms	1460sh	1460sh		1465m
1445s	1450ms	1440s	1450w	1455ms	1440m	1445ms	1445ms	1445ms	1445ms	1440s	1445s
1430sh	1435ms		1430s	1435s					1435ms		
					1425m	1423m	1420vs			1425s	1420s
1420ms	1420m	1415s	1410m	1415ms	1415w	1413s	1410sh	1415s	1415s		
1405w	1405w	1410w	1405sh	1410sh	1405w				1405ms		1410sh
A–B	A–B	A–B	A–B	A–B	A–B	B	A–B	A–B	A–B	B	A–B

Notes: The numbers in the columns are in cm^{-1}. The main peaks and preferable type of carbonation are underlined. *s* strong, *m* medium, *w* weak, *v* very, *sh* shoulder. The intensities are shown relatively to one another at each temperature. The total intensity of the v_3 CO_3^{2-} absorbance considerably decreased from 500 to 1100°C. So the absorbance at 1100°C was actually formed from the peaks of very weak intensities

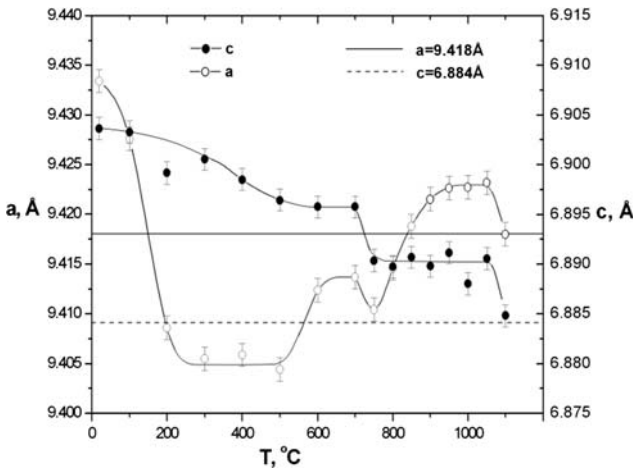

Fig. 2 Temperature dependences of the lattice constants

stoichiometric ones [12]. However, both lattice constants were found to increase. This could be caused by additional species which replaced Ca^{2+} and had considerably higher ionic radius than that of Ca^{2+} in order to surpass the contraction due to $CO_3^{2-} \rightarrow PO_4^{3-}$ substitution; e.g., the substitution of heavy ions for Ca^{2+} in HA is known to result in an increase both lattice constants [7]. This supposition turned out to be correct since the lattice constants, upon treating the products at RT–200°C, changed to values expected for a CHA, i.e., *a* values became lower and *c* values—slightly higher than the stoichiometric ones (Fig. 2). In addition, the treatment showed that the Ca^{2+} substituting ions easily released from the lattice, since even a gentle heating to 200°C resulted in a drastic reduction in *a* constant and its further stabilization at lowest values within 200–500°C.

The TG curve showed a total 6.85 wt% mass loss in the powder heated to about 960°C, and of 4.9 wt%, the majority of the mass, was lost within RT–500°C (Fig. 3). Hence, gaseous species released from the powder during the heating and, in particular, the reduction in *a* constant at RT–200°C could be associated with this process. However, the nature of the *a* reduction has not been ascertained from the data since a TG curve usually results from a release of species both adsorbed on the surface and evolved from the lattice. Besides, the mass loss might have been caused by a simultaneous release of a few kinds of species.

Mass loss during heating a HA-based product in the RT–500°C range is usually associated with the release of water. Adsorbed water was shown to liberate at RT–200°C and the so-called entrapped water—at 200–400°C [8]. However, the mode of the alterations in lattice constants (Fig. 2) points to another explanation of the mass to be lost. Really, depending on the synthesis conditions, different impurities might be incorporated into the lattice.

Mass spectrometrical examination of the powder answered the question. An assembled spectrum is shown in Fig. 4. As seen, the main gaseous products released were H_2O, CO_2 and the ones presented by 28 and 32 mass numbers; besides, some NH_x, CH_x and H_2 pieces were also detected at much lower partial pressures than those of the main gases. Water and carbon dioxide were the major components that evolved at RT–500°C. The curve of water evolution in the mass spectrum correlated excellently with the curve of mass loss rate (DTG) in TG examination at RT–300°C when the contribution of increasing CO_2 release was minor (Figs. 3 and 4). At higher temperatures, the TG and MSTA data were also consistent, however the DTG curve was approximately a sum of MSTA curves of all gases liberated.

Thus, the drastic decrease in *a* value was actually associated with release of H_2O and, to a less extent, of CO_2 slightly bonded in the lattice because of multitude imperfections in the structure. The characters of the observed

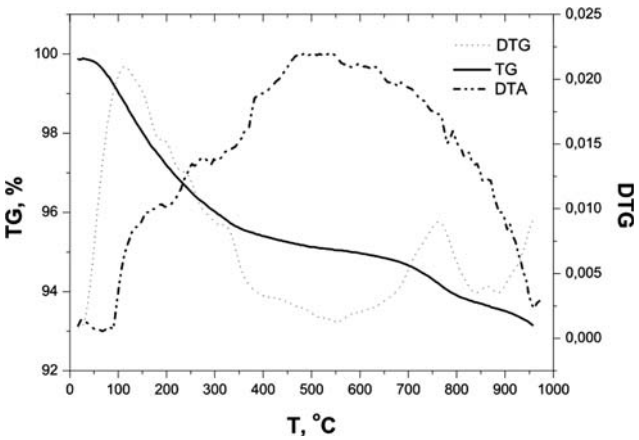

Fig. 3 TG-DTA examination of the powder

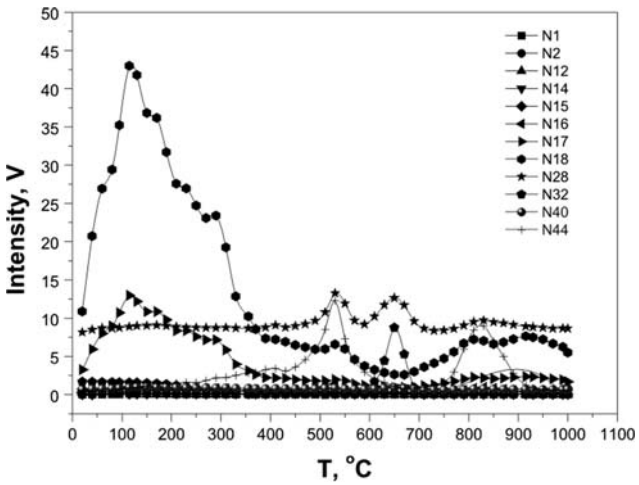

Fig. 4 The joined mass-spectra of gases liberated

diffraction maxima and DTA curve evidenced such imperfections. The diffraction maxima up to 700°C annealing temperature were considerably broadened. This was caused by both the nanosizes of grains and microstresses in them. The DTA curve had many small endopeaks that corresponded to individual evaporation processes which were also proved by both the DTG curve and peaks in mass spectra; however, on the whole, the DTA curve looked like a very broad exothermic maximum topped at about 500°C (Fig. 3). Appearance of the exomaximum could result from the generation of energy due to annealing the lattice defects which emerged in the synthesis process; such as extra vacancies, dislocations, nanoboundaries and incorporated foreign pieces. Of the pieces, liberation of water was found mainly to occur at lower temperatures (RT–200°C) than those observed earlier (200–400°C) [8]. This should not be considered a controversial fact. The nature of the substituent considerably effects its closest environment. The $CO_3^{2-} \rightarrow PO_4^{3-}$ substitution is known to cause the incorporation of some water and single charge ions into the lattice [7, 8, 10]. We used no Na^+ containing reactants [8], and consequently, another environment was formed around empty and/or substituted Ca^{2+} positions; different temperatures (lower—in our case) were needed to liberate the foreign pieces.

However, another explanation seems to be more suitable. Some NH_4^+ ions could have been incorporated into Ca^{2+}positions. Strong evidence for such an incorporation was found in considerably carbonated HA's precipitated in the presence of NH_4^+—containing reactants [19]. NH_4^+ ions in the reaction mixture could be hydrolyzed according to the reaction [20] $NH_4^+ + H_2O = H_3O^+ + NH_3 \uparrow$.

Hence, beside NH_4^+, the hydronium, H_3O^+, ions that resulted from the reaction could have been incorporated into the lattice of growing crystallites. The incorporation of H_3O^+ ions might have been more reliable, since the H_3O^+ ionic radius (1.09 Å) was larger than that of Ca^{2+} (0.99 Å), but much smaller than the ionic radius of NH_4^+ (1.43 Å) [7]. Nevertheless, these two kinds of substitution would result in increased lattice constants. While heating the products at temperatures higher than 96°C, the two substituents could decompose by the reactions $NH_4^+ = NH_3 \uparrow + H^+$ and $H_3O^+ = H_2O \uparrow + H^+$ with retaining a proton in a Ca^{2+} position to keep charge balance in the lattice [7, 21]. However, of the two possible volatile products, NH_3 and H_2O, the latter was only detected in the RT–200°C range when the lattice constants were decreasing. Figure 5 presents the ratio of M_{17}/M_{18} mass numbers of water during the heating the product. The ratio was constant and equaled 0.30 on average, a reference value for the mass spectrometer used and for dynamic mass spectrometers in general (the ratio for water is usually within 0.23–0.32 [22]). Hence, negligible ammonia was desorbed

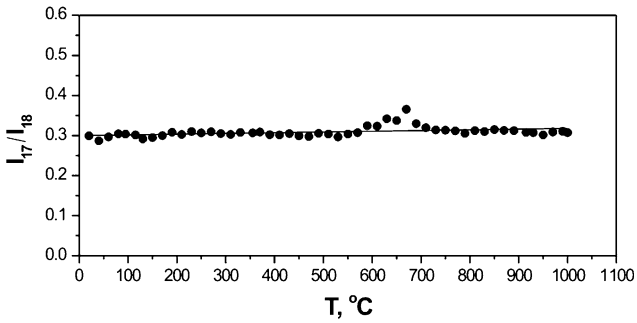

Fig. 5 The M_{17}/M_{18} ratio of water during heating the powder

during the whole heat treatment since the base peak of ammonia had appeared at mass number $M = 17$ and changed the ratio. Consequently, the abrupt decrease in a constant, most likely, was caused by release of peculiar "entrapped water" resulting from the decomposition of H_3O^+ ions incorporated into Ca^{2+} sites.

500–600°C. Thus, though the annealed powder lost the majority of adsorbed and unusually entrapped water, only a little carbon dioxide was released to 500°C (Figs. 2, 3 and 4). This was also consistent with IR data. The total ν_3 CO_3^{2-} absorbance (came from the square under the absorbance curve within 1400–1590 cm^{-1} [10]) slightly decreased upon annealing at RT–500°C and the peak characteristics of CO_3^{2-} ions in A- and B sites underwent little redistribution in relative intensities (Fig. 1b and Table 1). Consequently, the product annealed up to 500°C lost mainly the adsorbed carbon-containing groups and kept the majority of CO_3^{2-} groups incorporated into the lattice. The lattice constants were consistent with this conclusion as the a value (9.404 Å) and c value (6.896 Å) at 500°C were, respectively, lower and higher than the reference ones of HA, i.e., were typical of a CHA [12]. The characteristics of the treated powder started considerably changing at temperatures higher than 500°C. The IR-spectra of the powder annealed at 500–600°C displayed a few important features. First, the absorbances of OH^- groups both at 625 and 3560 cm^{-1} became clearly defined and increased in intensity with the increasing temperature (Figs. 1c and 6). Then, the AB- type transformed to B-type CHA. This followed from the disappearance of A-type absorbances (Table 1) and the shift of the ν_2 peak to 873 cm^{-1}; the peak was poorly resolved, but found within 875–880 cm^{-1} in all spectra at lower annealing temperatures. Finally, the CO_2 absorbance at about 2330 cm^{-1} first appeared with increased intensity at 500°C and disappeared at 600°C (Fig. 1c and the inset). Changes also occurred in lattice constants. While the c values slightly decreased, the a values markedly increased and both constants stabilized to 600°C (Fig. 2). Intensive release of CO_2 (the 28 M was a minor peak of 44 M) and water was observed in mass spectra (Fig. 4).

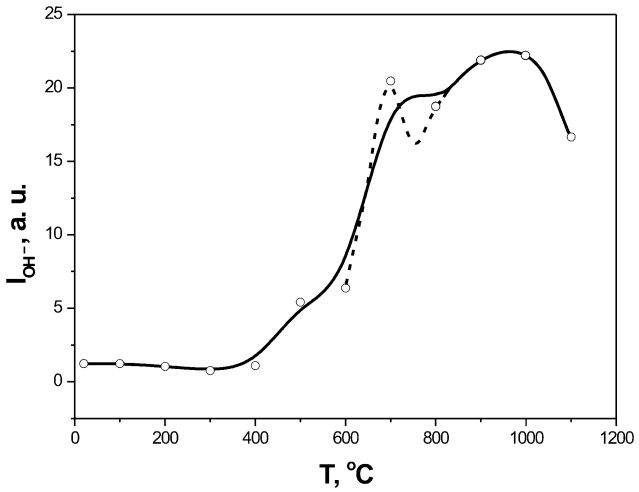

Fig. 6 Intensity evolution of the v_L librational mode of OH^-

All this data could be explained by the following processes. Of the reactions proposed for decomposition of the CO_3^{2-} groups located in A-sites, the next appear to be appropriate for consideration [15, 23]:

$$CO_3^{2-} + 2HPO_4^{2-} \rightarrow 2PO_4^{3-} + CO_2 \uparrow + H_2O \uparrow, \quad (1)$$

$$CO_3^{2-} \rightarrow CO_2 + O^{2-} \quad (2)$$

and

$$CO_3^{2-} + H_2O \rightarrow 2OH^- + CO_2 \uparrow . \quad (3)$$

The first reaction would not likely contribute to the observed increase in OH^- content (Fig. 6). Instead, a process similar to the one presented by reaction 1 proceeded at lower annealing temperatures, however, as the surface reaction

$HCO_3^- + HPO_4^{2-} = PO_4^{3-} + H_2O \uparrow + CO_2 \uparrow$

CO_2 pieces adsorbed from a water solution were usually in hydrolyzed form [20], and release of H_2O and CO_2, but negligible changes in OH^- content and lattice constants were observed (Figs. 2, 4 and 6). Additionally, presence of a hydrated layer incorporating partly HPO_4^{2-} and $CO_3^{2-}(HCO_3^-)$ pieces on the surface of precipitated HA-based particles has been recently proven [24, 25]; as such, besides surface carbonates, HPO_4^{2-} ions were found in the SCHA.

Careful examination of mass spectrometrical data of minor peaks revealed a few processes in the 500–600°C range. The low intensity $M = 12$ and $M = 16$ minor peaks of the CO_2 ($M = 44$) base peak had similar behavior and clearly demonstrated (e.g., in Fig. 7) that CO_2 released in two steps at around 500 and 570°C. Consequently, the CO_2 base peak and the $M = 28$ minor peak were not resolved because of high intensities (Fig. 4). Considering that the decomposition of CO_3^{2-} ions was accompanied by the appearance of OH^- ions in the lattice (Fig. 6), with no water released, and with low HPO_4^{2-} content in the initial powder (only a few weak peaks and shoulders of HPO_4^{2-} were present in the IR spectrum, see above), a process similar to reaction 1 could proceed at about 500°C according to

$$CO_3^{2-} + HPO_4^{2-} \rightarrow PO_4^{3-} + OH^- + CO_2 \uparrow . \quad (4)$$

The OH^- content that resulted from annealing the sample at 600°C changed little compared to that at 500°C (Fig. 6), despite the products released at 570°C that indicated a new portion of decomposed CO_3^{2-} (Fig. 7). The total CO_3^{2-} loss was also clearly seen in IR spectra since the absorbance area within 1400–1590 cm^{-1} due to v_3 CO_3^{2-} librational mode markedly decreased after annealing in the range. However, in contradiction to this, the intensity of the 873 cm^{-1} band usually associated with the v_3 CO_3^{2-} absorbance unexpectedly increased. This could have happened due to a superimposition of the v_3 CO_3^{2-} band and the Ca^{2+}–O^{2-} absorbance (875 cm^{-1}) [7] if O^{2-} ions formed instead of decomposed CO_3^{2-} groups in A-sites of the AB-type SCHA annealed to 600°C (Table 1). Hence, the CO_3^{2-} decomposition at 570°C occurred according to reaction 2.

Finally, a slight increase in H_2O liberation was detected at about 540°C between the two decarbonation peaks in mass spectra (Figs. 4 and 7). Since the water released was not associated with CO_3^{2-} decomposition in reactions 2 and 4, one could consider the increase to result from HPO_4^{2-} decomposition due to the reaction [26]

$$2HPO_4^{2-} \rightarrow P_2O_7^{4-} + H_2O \uparrow \quad (5)$$

For example, reaction 5 was known to occur during annealing a CdHA (mainly) within 350–650°C. The process was fast around 400°C and gradually slowed down as the temperature increased [26]. A similar trend of

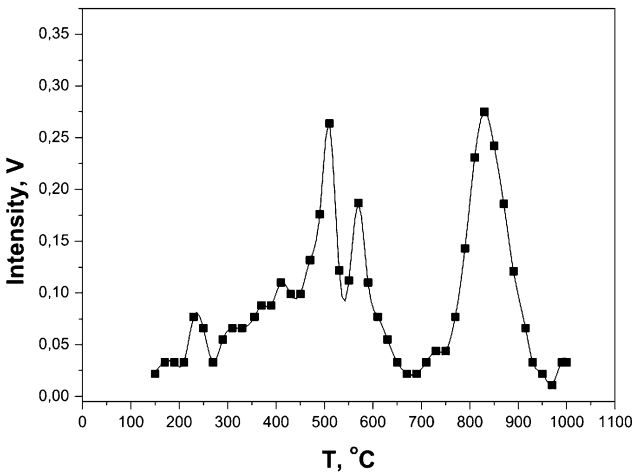

Fig. 7 Changes of $M = 12$ (carbon, C^+) minor peak during heating the sample

water liberation was observed in mass spectra at temperatures higher than about 400°C when the release of different kinds of bound water had finished (Fig. 4). Then, a weak but clearly defined peak was found in IR-spectra within 400–700°C. The peak located at around 720 cm^{-1} (715–735 cm^{-1}) and developed as the annealing temperature increased. The 720 cm^{-1} peak was usually associated with $P_2O_7^{4-}$ absorption [6, 7, 26]. Hence, at around 540°C (Fig. 7), in the temperature "slit" between the two decarbonation processes (while reaction 4 involving HPO_4^{2-} ions slowed down) more HPO_4^{2-} ions could take part in independently proceeding reaction 5 resulting in the slight splash in water liberation (Fig. 4).

Transformations of HPO_4^{2-} and CO_3^{2-} ions according to the above reactions would have resulted in a decrease in *a* constant since the decomposition products PO_4^{3-}, OH^- and O^{2-} had lower ionic radii than those of the parent ions (i.e., HPO_4^{2-} and CO_3^{2-}) [7]. Consequently, the observed increase of *a* value in the 500–600°C range could happen due to the formation of pyrophosphate ions $P_2O_7^{4-}$, which was expected to have a higher ionic radius than that of HPO_4^{2-} since it is composed of two PO_4^{3-} groups joined by a O^{2-} ion [20].

600–700°C. Two main observations were done in this annealing interval. Firstly, the content of OH^- groups abruptly increased in the lattice. We have considered the increase to happen due to an "outside" hydrolysis: temperatures above 600°C were high enough to intensify the hydroxylation of the product through dissociative adsorption (decomposition) of water vapor of the ambient atmosphere (air) on the surface and diffusion of the pieces formed (OH^- and H^+) into the bulk of powder particles [27]. Additionally, the majority of hexed sites were empty owing to the decarbonation occuring at 500–600°C. Due to this process, the intensity of OH^- absorbance at 700°C reached about 90% of the maximal value observed in this study (Fig. 6) without additional formation of hydroxyl ions by a lattice reaction as around 500°C. Secondly, intense gas liberation occurred peaking at 650°C (Fig. 4). However, no carbon containing gases were released: this displayed a deep minimum in the intensity of 12 M in the mass spectrum (Fig. 7). Besides, no water was released; the partial pressure of water was on the level of residual gases in the vacuum chamber (Fig. 4). The *a* and *c* values manifested negligible changes. The measured increase in *a* constant was within the experimental error (Fig. 2). This data was consistent with the fact that the maximal possible $P_2O_7^{4-}$ content in a typical CdHA subjected to heating had already formed at 700°C [26]. The base peaks in mass spectra were 28 and 32 M, and one would suppose that they resulted from decomposition of NO_3^- ions found in the powder. However, the decomposition of NO_3^- ions is known to occur within the 500–600°C range: e.g., $Ca(NO_3)_2$ starts decomposing at 500°C and melts at 560°C [20]. The measured ratios of 14/28 M and 16/32 M were not consistent with those of N_2 and O_2 [22]. Additionally, minor peaks of 2 M (H_2^+), 15 M (NH^+), and 16 M (NH_2^+) were observed to pass through a maximum simultaneously with peaks of 28 and 32 M at 650°C; possibly, also little ammonia was released since a weak splash was detected in the M_{17}/M_{18} dependence (Fig. 5). Although the bands at 2910 cm^{-1} and 2840 cm^{-1} (supposedly, of N_xH_y), were retained in spectra of samples annealed up to highest temperatures, they decreased in intensities almost two times in the spectrum of a sample treated at 700°C compared to those at 600°C. Most likely, a partial decomposition and/or reactions of the adsorbed pieces occurred. This was consistent with the main observation: negligible changes in *a* and *c* constants unambiguously point to primarily surface reactions on the SCHA particles.

700–800°C. Data obtained in this range turned out to be decisive in identifying the principal source of OH^- ions that step wisely increased in amount in the lattice during annealing the product from about 500 to 700°C. A slight decrease in intensity of the ν_L OH^- absorbance was observed in IR–spectrum of the sample treated at 800°C compared to that at 700°C, which pointed to some loss of OH^- groups in the lattice (Fig. 6). Besides, bands of free CO_2 within 2310–2340 cm^{-1} and CO_3^{2-} absorptions of an AB-type apatite appeared again (Fig. 1d, the inset, and Table 1). However, the most unexpected observation was that both lattice constants first decreased, then the *a* value increased and the *c* constant changed little (Fig. 2). Mass spectra showed the release of CO_2 and water, which increased in intensity with increasing temperature. However, the two curves of gas release were poorly associated (Fig. 4).

Filling the empty hexed sites with OH^- ions was expected to result in an increase in *a* values since the lattice became more perfect. However, only a negligible increase within 600–700°C, and then an abrupt decrease of the lattice constants in the 700–750°C range were observed. This pointed to a development of a stronger simultaneous process which affected the lattice dimensions than the filling. One could suppose that the process was the decomposition of $P_2O_7^{4-}$ ions, formed within 350–600°C, which is known to start in a slightly CdHA annealing above 650°C [26]. The corresponding reaction [26]

$$P_2O_7^{4-} + 2OH^- \rightarrow 2PO_4^{3-} + H_2O\uparrow \quad (6)$$

resulted in a release of water and decrease in OH^- content. Both these effects were observed. The water released curve demonstrated (Fig. 4) that the reaction actually started at about 650°C and intensified with increasing temperature. The developing reaction was the cause to why the OH^- content at 700°C could not reach its maximal value due to

outside hydrolysis, and then decreased at higher temperatures (most likely, the hypothetical dotted curve in Fig. 6 would best represent the alteration in OH^- content in the 600–800°C range). Since the ionic radius of $P_2O_7^{4-}$ was much higher than that of PO_4^{3-} (see above), the $P_2O_7^{4-}$ decomposition led to a decrease in lattice constants. This effect became stronger as the reaction developed. Therefore, it resulted in the observed limitation in increase of *a* value due to hydroxylation at 700°C and the drastic decrease of the lattice constants within 700–750°C (Fig. 2). Both effects would have continued at higher temperatures up to complete $P_2O_7^{4-}$ decomposition (likely, at about 900°C [26]), instead, the main decarbonation process started at 700°C, intensified with increasing temperature (Fig. 4) and interfered into reaction 6.

800–1050°C. The experimental data in this range was well consistent with one other. IR–spectra revealed a transition from an AB-type SCHA at 700°C to a B-type SCHA at 1000°C (Table 1). The mass spectra displayed a release of CO_2 at 750–950°C which peaked at about 830°C (Figs. 4 and 7). The *a* constant gradually increased and reached a plateau while the *c* constant oscillated around a mean within the experimental error, i.e., underwent minor changes. The lattice constants depend on the carbonate content in a B-type CHA: the more the carbonate the smaller the *a* value (a direct proportion), while the *c* value changes little [18]. In our case, a similar dependence was essentially observed. However, in a vice versa form: the less the carbonate the higher the *a* value (within 500–600 and 750–950°C) while the *c* value negligibly changed. This was an expected consequence from the known dependence. The nonlinear character of the found correlation could be associated with the type of HA carbonation: B-type in the case of direct dependence [18] and AB- type in the present study; besides, lattice reactions of other impurities affected the form of the dependence at 600–750°C.

Annealing at 800°C resulted in a mostly A-type apatite instead of a mostly B-type one at 700°C in the AB-type apatites on the whole (Table 1). This followed from a considerable decrease of the peak area within 1400–1500 cm^{-1} where the major B-type absorbances were located and alteration in the ν_2 CO_3^{2-} band. The band decreased in intensity almost twice and a doublet formed instead of the band at 875 cm^{-1} that looked like a single peak. Though poorly resolved, bands in the doublet were located at 873 and 878 cm^{-1} and had clearly different intensities in proportion of 0.4/1.0, respectively. Also, an intense absorbance of CO_2 around 2340 cm^{-1} appeared again as with the annealing at 500°C (Fig. 1d and the inset). All this testified to mainly CO_3^{2-} ions of the B-site decomposing. The decomposition products were likely released from the lattice through the hexed sites and formation of intermediate CO_3^{2-} groups in the A-position [15]. In this case, the observed increase in intensity of the major bands in the A-CO_3^{2-} range of 1500–1600 cm^{-1} (Table 1) would be associated with weakening the B-CO_3^{2-} bands. To answer the question more definitely, additional studying is required. Nevertheless, based on the data above, one could assert that the decomposition of CO_3^{2-} ions happened only in B-sites upon annealing the SCHA at 750 to 950°C.

We consider that the decomposition was caused by the reaction [15]

$$P_2O_7^{4-} + CO_3^{2-} \rightarrow 2PO_4^{3-} + CO_2 \uparrow . \quad (7)$$

Of the two PO_4^{3-} ions formed, one remained in the anionic site instead of the reacted $P_2O_7^{4-}$ ion and the other moved into the former B-site of the reacted CO_3^{2-} ion. However, the decomposition could also proceed in two stages. The first stage is reaction 2. The formed oxide ion is known to be very reactive [27] and, in the second stage, interacting with a pyrophosphate ion according to

$$P_2O_7^{4-} + O^{2-} \rightarrow 2PO_4^{3-} \quad (8)$$

would also result in two phosphate ions. In any case, the reactions would adjust the results of reaction 6 still proceeding in this range (see above). They appeared to be real, as no water, but phosphate ions were formed which explained the observed poor correlation of the curves for CO_2 and water released (Fig. 4).

The results of reactions 7 and/or 8 were consistent with the measured increase in *a*- and decrease in *c* values since the overall effect of the filling at the two anionic positions (formerly occupied by CO_3^{2-} and $P_2O_7^{4-}$) with native PO_4^{3-} ions led to perfection of the lattice and, therefore, to nearing of the lattice constants to those in stoichiometric HA. The overall effect turned out to be stronger than some decrease in *a* value because of $P_2O_7^{4-}$ decomposition by reaction 6 when annealing the SCHA above 700°C.

Despite two main ranges of CO_2 released (450–600°C and 750–950°C), CO_3^{2-} ions were not completely removed from the SCHA up to 1000°C (possibly, more durable annealing was needed and/or an inert treatment atmosphere).

Additionally, the IR-spectrum of a sample annealed at 1000°C clearly demonstrated that beside some CO_3^{2-} ions, traces of NO_3^-, CO_2, and (supposedly) N_xH_y were also present in the sample. Some decomposition products of these pieces could also be incorporated into the lattice. All this incorporated residue resulted in both slightly higher lattice constants (Fig. 2).

1050–1100°C. Unfortunately, the samples treated at temperatures above 1000°C were not as comprehensively characterized as those at lower temperatures. The TG-DTA and MSTA systems could be only operated up to about 1000°C. Nevertheless, some relevant data was obtained.

The intensities of OH^-groups in IR spectra decreased (Fig. 6) showing a dehydroxylation process starting in the SCHA [28]. Both lattice constants abruptly decreased to the stoichiometric values in HA (Fig. 2). Also, weak characteristic absorptions of beta tricalcium phosphate, β-TCP, at 950 and 1020 cm^{-1} appeared for samples treated at 1100°C. Additionally, both the ν_3- and ν_4 PO_4^{3-} absorbtions markedly broadened indicating to some fine phase appearing in the sample (Fig. 1e). However, the XRD pictures only revealed a single apatite phase, the same as in all samples annealed before. Hence, the slightly carbonated (i.e., nonstoichiometric) HA which also incorporated other impurities in trace amounts decomposed to a stoichiometric HA and some portion of β-TCP. This portion was too small to be detected by the XRD method (the sensitivity of about 0.5 wt% for β-TCP). These observations are additional reasons for the above conclusions on the nature and thermal evolution of the impurities in the SCHA.

In the above consideration, the TG date for annealing temperatures higher than 500°C were not immediately examined since the processes in this range had to first be clarified. After clarification, let us to turn to this data. Mass loss in a CHA at 500–900°C is usually associated with decomposition of CO_3^{2-}ions [12, 15]. Following this, the mass loss of 1.6 wt% measured within 500–900°C (Fig. 3) corresponded to decomposition of about 2.2 wt% of CO_3^{2-} ions since about 0.6 wt% of O^{2-} remained in the lattice. Even considering that all the O^{2-} ions were accumulated in A-sites and the Ca^{2+} and PO_4^{3-} positions were completely filled, this amount plays too small a part in the hydrolysis of such a CHA losing its carbonate groups (comparing to 3.3 wt% of OH^- in a stoichiometric HA since joining H^+ ions would produce a minor increment in the 0.6 wt% of O^{2-} mass). Moreover, considerable water release comparable (by partial pressure) with that of CO_2 occurred in the range and the mass loss at 500–600°C was owing mainly to a surface reaction (Fig. 4). Besides, the OH^- sites were almost fully filled before annealing at 800°C when the major part of incorporated CO_3^{2-} decomposed. All this displayed that even a smaller part, than the hypothetically considered 0.6 wt%, was really associated with O^{2-} ions in the 2.2 wt% mass loss. Two important consequences could be derived from this data: (i) the reliability of the above conclusion that the O^{2-} pieces resulted from CO_3^{2-} decomposition both due to the thermal destruction and/or a chemical reaction played a minor role in hydrolysis of the SCHA; (ii) analysis of TG data for a SCHA, incorporated several impurities, as in the study, without parallel examination of mass spectrometric and/or dynamic IR–spectroscopic observations, may lead to confusing results.

Finally, two more remarks. The first, an enriched set of bands in the ν_3 CO_3^{2-} range was found in this study with respect to the one observed earlier [6, 7, 12]. We are not sure whether all the bands were associated with CO_3^{2-} ions: several additional impurities were present in the SCHA. Therefore, the found bands are presented in Table 1 just as those detected in the ν_3 CO_3^{2-} range. Nevertheless, one should pay attention to (i) that almost the complete set was retained to the highest annealing temperatures, and (ii) that comparing the set data with the appropriate known characteristics showed a strong coincidence. E.g., an AB–type HA synthesized under conditions very close to those in this study manifested bands in the ν_3 CO_3^{2-} range at 1570, 1545, 1504, 1498, 1466, 1455 and 1410 cm^{-1} upon heat treatment at 900°C [12]. This group is the main part of the set detected in the present study for the sample annealed at 900°C, and the band characteristics excellently (within the experimental error) coincide (Table 1).

The second, analysis of the data in Table 1 gave some suggestion on the mechanism of decarbonation. Following the development of the major CO_2 peak in the 750–950°C range (Figs. 4 and 7), one could clearly see that the kind of carbonation changed from a mainly B-type (700°C) to a mainly B-type again (900–1000°C) after a mainly A-type (800°C) in the samples annealed. The A-type was approximately observed at the temperature of maximal CO_2 release (830°C). Simultaneously, some CO_2 trapped in the sample was found (Fig. 1, the inset). A similar process, most likely, happened in the 450–600°C range (Table 1) when in both IR-and mass spectra a CO_2 peak was detected at 500°C (Figs. 1, the inset, and 4, 7). This data was consistent with the earlier observations and suggests that the decarbonation process in B-sites could occur via the release of decomposition product(s) through hexed channels and formation some temporary CO_3^{2-} groups in A-sites due to a CO_2 intermediary [29].

4 Conclusions

1. Lattice and surface reactions of impurities and their influence on the structure of a slightly carbonated hydroxyapatite (SCHA) were comprehensively studied in a wide temperature range (RT–1100°C). The SCHA, synthesized by a conventional wet method using ammonium contained parent reagents at a relatively high temperature (96°C), contained small amount of carbonate groups (A- and B-sites) and minor crystallization water. Some cationic and anionic sites were also filled with NH_4^+, H_3O^+ and HPO_4^{2-} ions, respectively. H_2O, HPO_4^{2-}, CO_3^{2-} (or, most likely, HCO_3^-), NO_3^- and (apparently) N_xH_y pieces were adsorbed on the surface of crystallites. Stepwise annealing of the SCHA in air displayed a variety of reactions among the impurities.

In the RT–500°C annealing range, when the adsorbed and crystallization water usually are released, the *a* lattice constant abruptly decreased to about 200°C from an enlarged value (9.433 Å) to a lower one (9.405 Å) compared to the stoichiometric constant of HA (9.418 Å) and was then practically invariable at 200–500°C, i.e., changed conversely to the known dependences in this two subranges [8]. This was associated with the thermal decomposition of H_3O^+ ions incorporated into the lattice during synthesis owing to the hydrolysis of NH_4^+ ions by the reaction $NH_4^+ + H_2O = H_3O^+ + NH_3\uparrow$. The decomposition occurred according to the reaction $H_3O^+ = H^+ + H_2O\uparrow$ and resulted in H^+ ions remaining in cationic sites.

CO_2 liberations were observed at 450–600 and 700–950°C. An increase in *a* constant was measured in both cases. Within 450–600°C, a two-step CO_2 liberation was firstly observed. At about 500°C, the CO_2 release happened due to the reaction $CO_3^{2-} + HPO_4^{2-} \rightarrow PO_4^{3-} + OH^- + CO_2\uparrow$ and resulted in a partial filling of the hexed sites with OH^- ions. At about 570°C, the other step in CO_2 release occurred owing to the reaction $CO_3^{2-} \rightarrow CO_2\uparrow + O^{2-}$. Simultaneously, the decomposition of lattice HPO_4^{2-} ions proceeded in this region as $2HPO_4^{2-} \rightarrow P_2O_7^{4-} + H_2O\uparrow$ which resulted in H_2O liberation and the first increase in *a* value.

Two surface processes took place at 600–700°C. The first one was the hydrolysis of the SCHA due to atmospheric water vapor which resulted in complete filling of the hexed sites by OH^- ions. The other process was a reaction of the adsorbed impurities, which involved NO_3^- and N_xH_y pieces, and led to an intense release of gas at about 650°C, with no carbon containing volatile products.

The decomposition of $P_2O_7^{4-}$ ions, formed in the lattice at lower annealing temperatures, happened by the reaction $P_2O_7^{4-} + 2OH^- \rightarrow 2PO_4^{3-} + H_2O\uparrow$ within 700–750°C and resulted in a drastic decrease of both lattice constants.

The major lattice reaction in the 750–950°C range was the decomposition of CO_3^{2-} ions of mainly B-sites. This resulted in the release of CO_2which peaked at 830°C. The *a* constant gradually increased again and reached a plateau at 950–1050°C having a value higher than that of stoichiometric HA because of trace impurities still retaining in the lattice. This second increase in *a* constant was associated with formation of PO_4^{3-} groups due to the reactions of CO_3^{2-} and/or O^{2-} ions (resulted from the CO_3^{2-} thermal decomposition) with the rest of $P_2O_7^{4-}$ ions in the lattice according to $CO_3^{2-} + P_2O_7^{4-} \rightarrow 2PO_4^{3-} + CO_2\uparrow$ and/or $O^{2-} + P_2O_7^{4-} \rightarrow 2PO_4^{3-}$, respectively.

A dehydroxylation process started with annealing above 1000°C. Little amount of β-TCP, not detectable by XRD but detected by IR-method, formed in the SCHA up to 1100°C. Both lattice constants decreased to the reference values of HA. Hence, the annealed product transformed to a mixture of stoichiometric HA and a minor portion of β-TCP.

2. The decomposition of CO_3^{2-} groups happened due to two reactions with impurity ions entrapped into the lattice and thermal destruction. The decarbonation in A-sites occurred at much lower temperatures (450–600°C) than that in B-sites (700–950°C) and was first shown to proceed in two stages: by an impurity reaction—around 500°C, and through the thermal destruction—at 570°C. A redistribution of CO_3^{2-} groups in A- and B-sites was observed upon annealing above 500°C.
3. The amount of OH^- groups resulted from the lattice reactions turned out to be not enough for the total filling the hexed sites in the lattice. Drastic filling of the sites by hydroxyl ions at 600–700°C occurred mainly due to hydrolysis of the SCHA by water molecules of air.
4. The mass loss measured by TG within 500–900°C was shown to happen due to liberation of gaseous products of different nature. Hence, data on CO_3^{2-} content in a CHA usually computed from the TG measurement in this range, assuming the mass loss solely as a result of CO_3^{2-} decomposition, could be correctly derived only by considering data on the nature of products liberated.

References

1. Dry ME, Beebe RA. Adsorption studies on bone mineral and synthetic hydroxyapatite. J Phys Chem. 1960;64:1300–4. doi:10.1021/j100838a042.
2. Bett JA, Christner LG, Hall KW. Studies of the hydrogen held by solids. XII. Hydroxyapatite catalysts. J Am Chem Soc. 1967;89(22):5535–41. doi:10.1021/ja00998a003.
3. Nagai M, Nishino T. A new type of CO_2 gas sensor comprising porous hydroxyapatite ceramics. Sens Actuators. 1988;15:145–51. doi:10.1016/0250-6874(88)87004-5.
4. Jeanjean J, Rouchaud JC, Tran L, Fedoroff M. Sorption of uranium and other heavy metals on hydroxyapatite. J Radioanal Nucl Chem Lett. 1995;201(6):529–39. doi:10.1007/BF02162730.
5. Reichert J, Binner JGP. An evaluation of hydroxyapatite-based filters for removal of heavy metal ions from aqueous solutions. J Mater Sci. 1996;31:1231–41. doi:10.1007/BF00353102.
6. Ratner BD, et al. Biomaterials science: an introduction to materials in medicine. In: Ratner BD, et al., editors. California: Elsevier Academic Press; 2004.
7. Narasaraju TS, Phebe DE. Some physico-chemical aspects of hydroxyapatite. J Mater Sci. 1996;31:1–21. doi:10.1007/BF00355120.

8. LeGeros RZ, Bonel G, Legros R. Types of "H_2O" in human enamel and in precipitated apatites. Calcif Tissue Res. 1978; 26:111–8. doi:10.1007/BF02013245.
9. Feki HE, Savariault JM, Salah BA. Structure refinements by the Rietveld method of partially substituted hydroxyapatite: $Ca_9Na_{0,5}(PO_4)_{4,5}(CO_3)_{1,5}(OH)_2$. J Alloy Comp. 1999;287:114–20. doi:10.1016/S0925-8388(99)00070-5.
10. Rehman I, Bonfield W. Characterization of hydroxyapatite and carbonated apatite by photo acoustic FTIR spectroscopy. J Mater Sci Mater Med. 1997;8:1–4. doi:10.1023/A:1018570213546.
11. Zyman Z, Rokhmistrov D, Ivanov I, Epple M. The influence of foreign ions on the crystal lattice of hydroxyapatite upon heating. Mat-wiss Werkstoftech. 2006;37(6):530–2. doi:10.1002/mawe.200600032.
12. Gibson IR, Bonfield W. Novel synthesis and characterization of an AB-type carbonate-substituted hydroxyapatite. J Biomed Mater Res. 2002;59:697–708. doi:10.1002/jbm.10044.
13. Mortier A, Lemaitre J, Rouxhet PG. Temperature-programmed characterization of synthetic calcium-deficient phosphate apatites. Thermochim Acta. 1989;143:265–82. doi:10.1016/0040-6031(89)85065-8.
14. Anderson CW, Beebe RA, Kittelberger JS. Programmed temperature dehydration studies of octacalcium phosphate. J Phys Chem. 1974;78(16):1631–5. doi:10.1021/j100609a007.
15. Dowker SEP, Elliott JC. Infrared study of trapped carbon dioxide in thermally treated apatites. J Solid State Chem. 1983;47:164–73. doi:10.1016/0022-4596(83)90005-1.
16. Fowler BO, Moreno EC, Brown WE. Infra-red spectra of hydroxyapatite, octacalcium phosphate and pyrolysed octacalcium phosphate. Arch Oral Biol. 1966;11:477–92. doi:10.1016/0003-9969(66)90154-3.
17. Berry EE, Baddiel CB. Some assignments in the infra-red spectrum of octacalcium phosphate. Spectrochimica Acta. 1967;23A:1781–92.
18. LeGeros RZ. Effect of carbonate on the lattice parameters of apatite. Nature. 1965;4982:403–4. doi:10.1038/206403a0.
19. Vignoles M, Bonel G, Young RA. Occurrence of nitrogenous species in precipitated B-type carbonated hydroxyapatites. Calcif Tissue Int. 1987;40:64–70. doi:10.1007/BF02555707.
20. Glinka NL. General chemistry. Leningrad: Chemistry Press; 1977.
21. Simpson DR. Substitutions in apatite: I potassium-bearing apatite. Am Mineral. 1968;53:432–44.
22. Cornu A, Massot R. Compilation of mass spectral data. London: Heyden and Son Ltd; 1974.
23. Apfelbaum F, Diab H, Mayer I, Featherstone JDB. An FTIR study of carbonate in synthetic apatites. J Inorg Biochem. 1992;45:277–82. doi:10.1016/0162-0134(92)84016-G.
24. Cazalbou S, Eichert D, Ranz X, Drouet C, Combes C, Harmand MF, et al. Ion exchange in apatites for biomedical applications. J Mater Sci Mater Med. 2005;16:405–9. doi:10.1007/s10856-005-6979-2.
25. Jäger C, Welzel T, Meyer-Zaika W, Epple M. A solid-state NMR investigation of the structure of nanocrystalline hydroxyapatite. Magn Reson Chem. 2006;44:573–80. doi:10.1002/mrc.1774.
26. Berry EE. The structure and composition of some calcium-deficient apatites.—I and II. J Inorg Nucl Chem. 1967;29:317–27, 1585–90.
27. Trombe JC, Montel G. Some features of the incorporation of oxygen in different oxidation states in the apatite lattice. J Inorg Nucl Chem. 1978;40:15–21. doi:10.1016/0022-1902(78)80298-X.
28. Kijima T, Tsutsumi M. Preparation and thermal properties of dense polycrystalline oxyhydroxyapatite. J Am Ceram Soc. 1979; 62:455–60. doi:10.1111/j.1151-2916.1979.tb19104.x.
29. Holcomb DW, Young RA. Thermal decomposition of human tooth enamel. Calcif Tissue Int. 1980;31:189–201. doi:10.1007/BF02407181.